

28

Imperfections

TABLE OF CONTENTS

	Page
§28.1. No Body is Perfect	28-3
§28.2. The Imperfect Hinged Cantilever	28-3
§28.2.1. Equilibrium Analysis	28-3
§28.2.2. Critical Point Analysis	28-3
§28.2.3. Discussion	28-4
§28.3. The Imperfect Propped Cantilever	28-5
§28.4. Parametrizing Imperfections	28-7
§28.5. Imperfection Sensitivity at Critical Points	28-8
§28.5.1. Limit Point	28-9
§28.5.2. Asymmetric Bifurcation	28-9
§28.5.3. Stable Symmetric Bifurcation	28-10
§28.5.4. Unstable Symmetric Bifurcation	28-10
§28.6. Extensions: Multiple Bifurcation, Continuous Systems	28-10
§28. Exercises	28-12

§28.1. No Body is Perfect

In the previous four Chapters we have been concerned with the behavior of *geometrically perfect* structures. For the geometrically nonlinear analysis of slender structures, such as those used in aerospace products, we must often take into account the presence of *imperfections*. It is useful to distinguish two type of imperfections, one associated with the physical structure, the other with the computational model.

Physical imperfections. Physical imperfections may be categorized into fabrication and load imperfections. Real structures inevitably carry geometric imperfections inherent in their manufacture. In addition, loads on structural members that carry primarily compressive loads, such as columns and cylindrical shells, are not necessarily centered. The load-carrying capacity of certain classes of structures, notably thin shells, may be significantly affected by the presence of physical imperfections. We shall see that high sensitivity to the presence of small imperfections is a phenomenon associated with certain types of critical points. Structures that exhibit high sensitivity are called *imperfection sensitive*.

Numerical imperfections. Imperfections may be incorporated in the computational model for various reasons. Numerical imperfections may be used to either simulate actual physical imperfections or to “trigger” the occurrence of certain types of response. One common application of numerical imperfections is in fact to “nudge” the structure along a post-bifurcation path, as in Exercises 21.2 and 21.3.

We begin the study of the effect of imperfections through a simple yet instructive one-degree-of-freedom example: the imperfect hinged cantilever.

§28.2. The Imperfect Hinged Cantilever

We take up again the critical-point analysis of the hinged cantilever already studied in §25.5. But we assume that this system is *geometrically imperfect* in the sense that the rotational spring is unstrained when the rigid bar “tilts” by a small angle ϵ with the vertical. By varying ϵ we effectively generate a *family* of imperfect systems that degenerate to the perfect system when $\epsilon \rightarrow 0$.

Denoting again the total rotation from the vertical by θ as shown in Figure 28.1, the strain energy of the imperfect system can be written

$$U(\theta, \epsilon) = \frac{1}{2}k(\theta - \epsilon)^2. \quad (28.1)$$

The potential energy of the imperfect system is

$$\Pi(\theta, \lambda, \epsilon) = U - V = \frac{1}{2}k(\theta - \epsilon)^2 - fL(1 - \cos \theta) = k \left[\frac{1}{2}(\theta - \epsilon)^2 - \lambda(1 - \cos \theta) \right], \quad (28.2)$$

in which as before we take $\lambda = fL/k$ as dimensionless control parameter.

§28.2.1. Equilibrium Analysis

The equilibrium equation in terms of the angle θ as degree of freedom is

$$r = \frac{\partial \Pi}{\partial \theta} = k(\theta - \epsilon - \lambda \sin \theta) = 0. \quad (28.3)$$

Therefore, the equilibrium path equation of an imperfect system is

$$\lambda = \frac{\theta - \epsilon}{\sin \theta}. \quad (28.4)$$

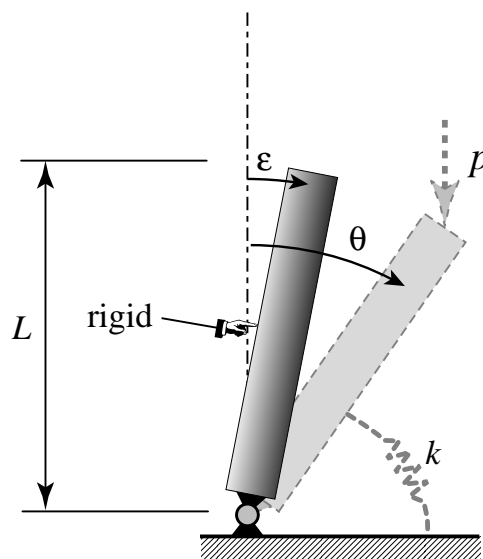


Figure 28.1. The imperfect hinged cantilever. The imperfection parameter is the initial tilt angle ϵ .

§28.2.2. Critical Point Analysis

The first-order incremental equation in terms of θ is the same as in Chapter 25:

$$K\dot{\theta} - q\dot{\lambda} = 0, \quad (28.5)$$

where

$$K = \frac{\partial r}{\partial \theta} = k(1 - \lambda \cos \theta), \quad q = \frac{\partial r}{\partial \theta} = k \sin \theta. \quad (28.6)$$

We have stability if $K > 0$, that is

$$1 - \lambda \cos \theta > 0, \quad (28.7)$$

and instability if $K < 0$, that is

$$1 - \lambda \cos \theta < 0. \quad (28.8)$$

Critical points are characterized by $K(\lambda_{cr}) = 1 - \lambda_{cr} \cos \theta = 0$, or

$$\lambda_{cr} = \frac{1}{\cos \theta}. \quad (28.9)$$

On equating this value of λ with that given by the equilibrium solution (28.4) we obtain

$$\theta - \epsilon = \tan \theta. \quad (28.10)$$

This relation characterizes the *locus of critical points* as ϵ is varied. It is not difficult to show that these critical points are limit points if $\epsilon \neq 0$ (imperfect systems) and a bifurcation point if and only if $\epsilon = 0$ (perfect system).

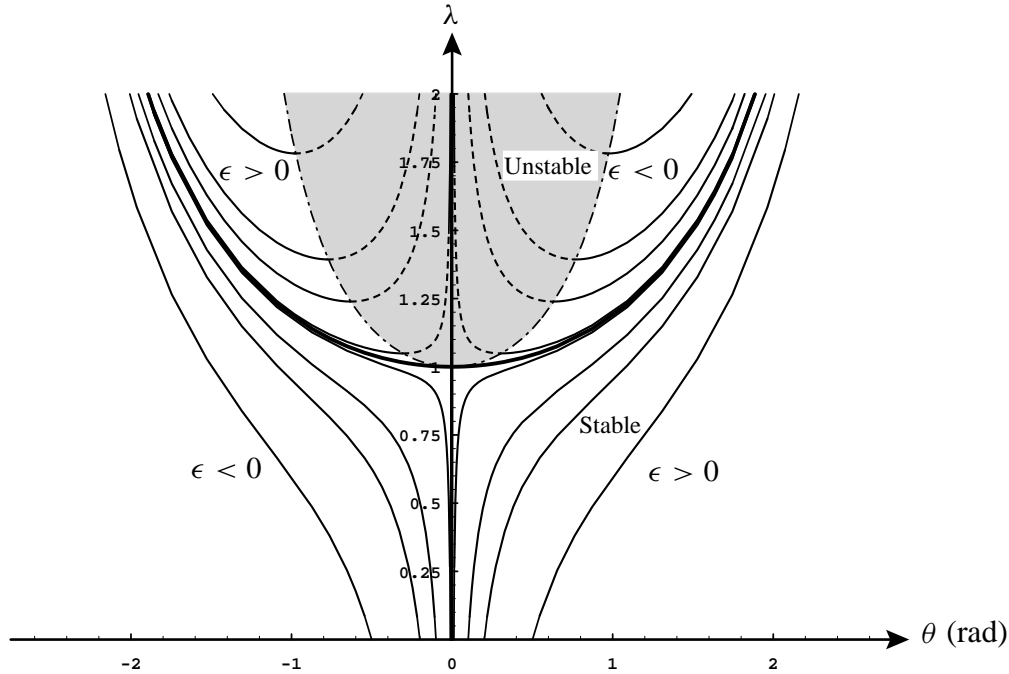


Figure 28.2. Equilibrium paths of the imperfect ($\epsilon \neq 0$) and perfect ($\epsilon = 0$) hinged cantilever.

§28.2.3. Discussion

The response of this family of imperfect systems is displayed in Figure 28.2.

In this Figure heavy lines represent the response of the perfect system whereas light lines represent the responses of imperfect systems for fixed values of ϵ . Furthermore continuous lines identify stable equilibrium path portions whereas broken lines identify unstable portions. We see that systems with a positive ϵ give equilibrium paths in two opposite quadrants while systems with a negative ϵ give equilibrium paths in the remaining two quadrants. The equilibrium paths of the imperfect systems collapse onto the equilibrium paths of the perfect system as ϵ goes to zero. The locus of critical-point equilibrium states given by (28.10) separates the stable and unstable domains and is shown in Figure 28.2 as curve ss .

We see that a given imperfect system loaded from its unstrained state will give rise to a constantly rising path so that no instability is encountered; the deflections merely growing more rapidly as the critical load of the perfect system is passed. In addition to this *natural* equilibrium path an imperfect system will also have a *complementary* path which lies in the opposing quadrant. However, this path (partly stable and partly unstable) will not be encountered in a natural loading process that starts from $\lambda = 0$.

The response shown in Figure 28.2 is well known to structural engineers and is exhibited by the familiar Euler column which is taught in elementary courses of mechanics of materials. In §28.5 it is shown that this behavior is characteristic of systems that possess a stable-symmetric bifurcation point.

§28.3. The Imperfect Propped Cantilever

The perfect propped cantilever is shown in Figure 28.3. It differs from the hinged cantilever in that it is supported by an ordinary (rectilinear) spring of stiffness k attached to the top. An imperfect version is shown in Figure 28.4, where the initial horizontal displacement ϵL defines the imperfection parameter ϵ .

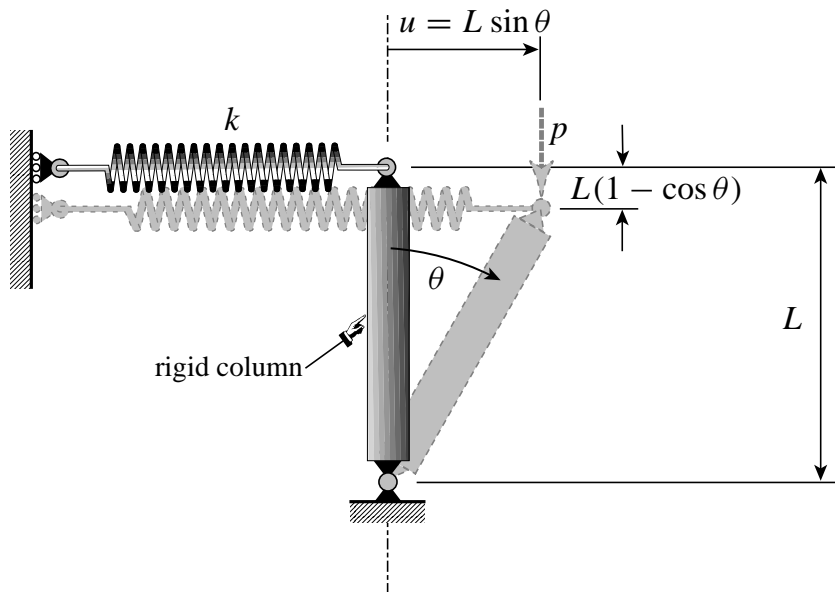


Figure 28.3. The perfect propped cantilever.

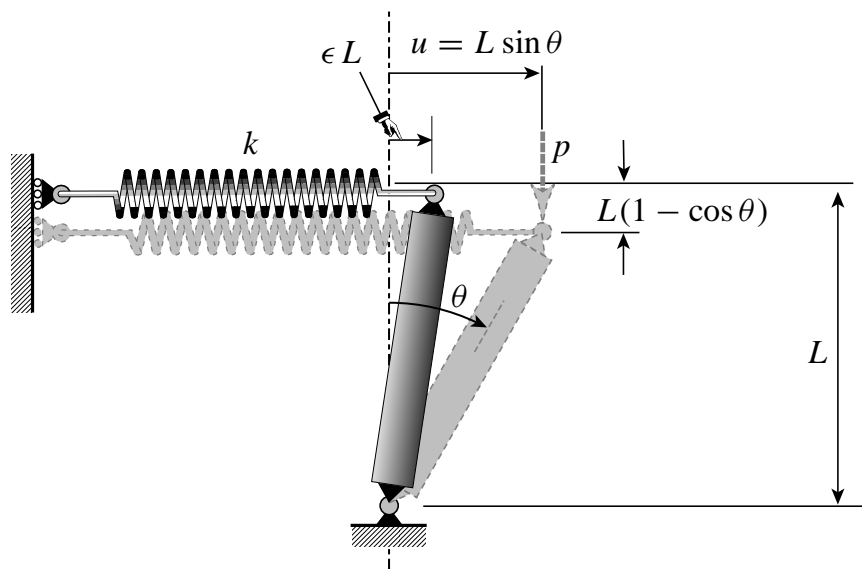


Figure 28.4. The imperfect propped cantilever. The imperfection parameter is ϵ , where ϵL is the displacement from the vertical at which the rectilinear spring is unstrained.

The potential energy of the imperfect structure is

$$\Pi(u, f) = U - V = \frac{1}{2}k(u - \epsilon L)^2 - fL(1 - \cos \theta) = \frac{1}{2}k(u - \epsilon L)^2 - fL\sqrt{1 - (u/L)^2} \quad (28.11)$$

where $u = L \sin \theta$ is the total horizontal displacement from the vertical, and a constant term has been dropped from V . It is convenient to take the ratio $\lambda = fL/k$ as dimensionless control parameter and $\mu = u/L$ as the

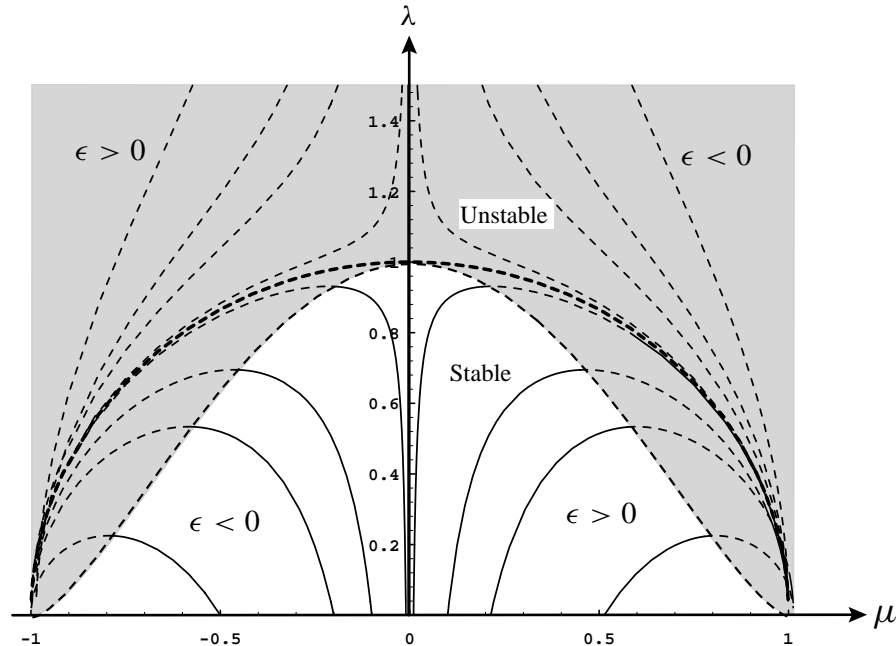


Figure 28.5. Equilibrium paths of the imperfect ($\epsilon \neq 0$) and perfect ($\epsilon = 0$) propped cantilever.

dimensionless state variable. Then the potential energy, upon dividing by kL^2 , becomes

$$\Pi(\mu, \lambda) = \frac{1}{2}(\mu - \epsilon)^2 - \lambda\sqrt{1 - \mu^2} \quad (28.12)$$

The residual equation in terms of μ , λ and the imperfection parameter is

$$r(\mu, \lambda, \epsilon) = \mu - \epsilon - \lambda \frac{\mu}{\sqrt{1 - \mu^2}} = 0 \quad (28.13)$$

Carrying out the analysis as in the previous section, one finds the response paths depicted in Figure 28.5. The important difference is that the bifurcation point is now of unstable-symmetric type. The equilibrium paths that emerge from the unloaded state of the imperfect systems are no longer rising but exhibit limit-point maxima that may be viewed as failure loads. These limit points occur at *lower* loads than the bifurcation load of the perfect structure.

Therefore, the load-carrying capacity of the propped cantilever is adversely affected by the imperfection, and the structure is said to be *imperfection-sensitive*.

§28.4. Parametrizing Imperfections

The treatment of imperfections in the foregoing two examples illustrates many features that recur in more complex cases. *Imperfect systems* are derived as *perturbations* of the perfect system. Imperfections in real structures are seldom known precisely. They are usually random quantities that can be rigorously treated only by stochastic techniques. Such a treatment, however, would be hopelessly expensive in nonlinear systems. A more practical deterministic approach consists of looking at a *parametrized family* of imperfect systems characterized by a dimensionless *imperfection parameter* ϵ .

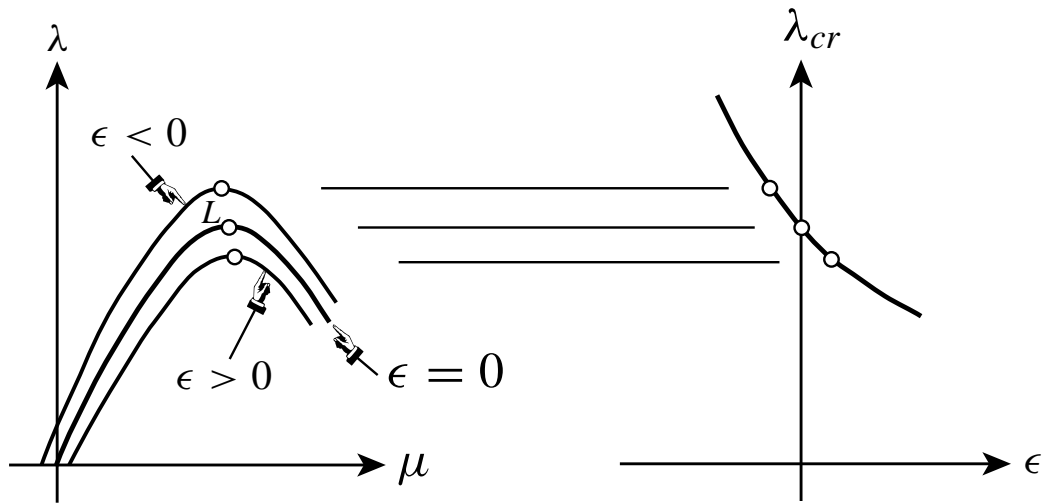


Figure 28.6. Effect of initial imperfections at a limit point.

The system corresponding to $\epsilon = 0$ is called the *perfect system*. Systems corresponding to $\epsilon \neq 0$ are described as *imperfect systems*. Parameter ϵ is inserted in the potential energy $\Pi(\mathbf{u}, \lambda, \epsilon)$. For each fixed ϵ the analysis proceeds along the usual lines: residual equilibrium equations, first order incremental equations, finding critical points, and so on.

The physical interpretation of the parameter depends on the type of structure. For example, in the analysis of thin shells whose thickness is accurately controlled a natural choice would be the ratio of the expected imperfection amplitude to the thickness. If the thickness itself may vary locally about its nominal value — as it would happen, for example, in reinforced concrete shells — the thickness variation may be taken as the imperfection parameter. In general we may say that the choice of parameter is tied up to the fabrication method whereas the value of the parameter is determined by fabrication or construction quality control. In the case of mass-produced systems imperfection data is sometimes available from actual field measurements.

§28.5. Imperfection Sensitivity at Critical Points

The effect of imperfections on the load-carrying capacity of a structure that fails at a critical point may drastically vary according to the type of critical point. Structures whose failure loads are substantially reduced by imperfections are called *imperfection sensitive*. In this Chapter we review the question of sensitivity for the four types of critical points introduced in Chapter 23, using typical response plots.

In the following two-dimensional response plots, the dimensionless control parameter λ is plotted against a representative state parameter. This λ is assumed to be a *load multiplier* or *load factor* that characterizes the strength of the structure. Following the same conventions as in the example of §25.2 heavy lines represent the equilibrium path of the *perfect system* while light lines represent the equilibrium paths of *imperfect systems*. Furthermore continuous lines represent *stable* equilibrium path segments whereas broken lines represent *unstable* equilibrium segments.

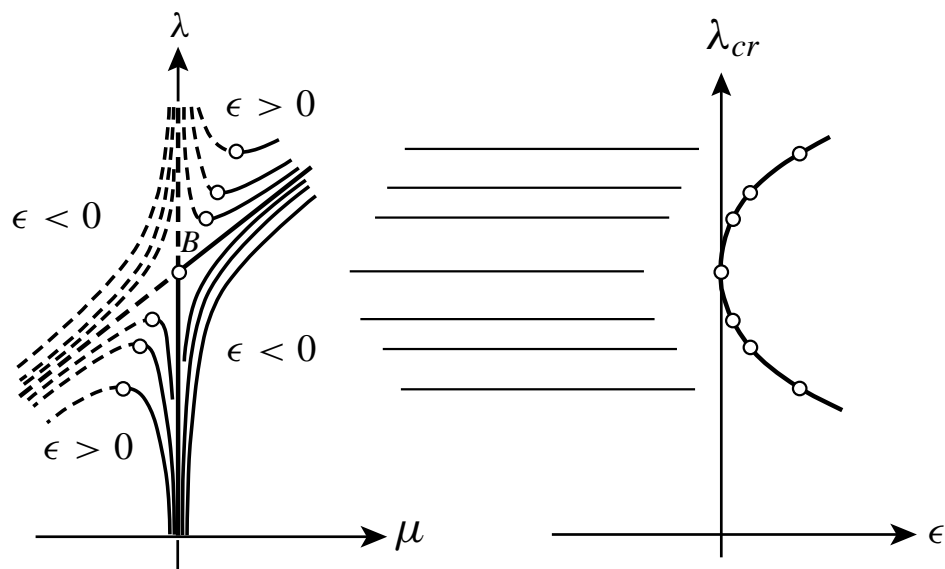


Figure 28.7. Effect of initial imperfections at an asymmetric bifurcation point.

§28.5.1. Limit Point

Figure 28.6 pertains to a limit point. We see that the response of the imperfect system is not dissimilar from that of the corresponding perfect system. The peak or *failure load* measured by λ_{cr} varies quasi-linearly with the imperfection parameter ϵ and this variation $\lambda_{cr}(\epsilon)$ is shown in the right-hand diagram of Figure 28.6. As can be observed the function $\lambda_{cr}(\epsilon)$ has normally a finite and nonzero slope and exhibits no singular behavior as $\epsilon \rightarrow 0$. We may characterize a system that fails at a limit point typified by the response of Figure 28.6 as being *mildly imperfection sensitive*.

§28.5.2. Asymmetric Bifurcation

Typical pictures for an asymmetric point of bifurcation are shown in Figure 28.7. Now we see that imperfections play a far more significant role in changing the critical-point response of the system than in the previous case.

For a small positive¹ value of ϵ , the system loses stability at a limit point that corresponds to a drastically reduced value of λ . On the other hand a system with a small negative value of ϵ apparently exhibits no instability in the vicinity of the bifurcation point and follows a stable rising path. We might note, however, that this continuously rising path travels a region of metastability and consequently it may not be reliable in the presence of small dynamic disturbances.

The variation of the failure load factor λ_{cr} with the imperfection parameter ϵ , shown in the right-hand diagram, is now of considerable interest. For positive imperfections the function $\lambda_{cr}(\epsilon)$ is locally parabolic, having no singularities as $\epsilon \rightarrow 0$ but an infinite slope as shown. Thus there is an *extreme sensitivity* to initial positive imperfections. Since systems with negative imperfections display no local failure loads their “buckling” is characterized by a more rapid growth of the deflections as the

¹ Positive in the sense that it reinforces the bifurcation phenomenon.

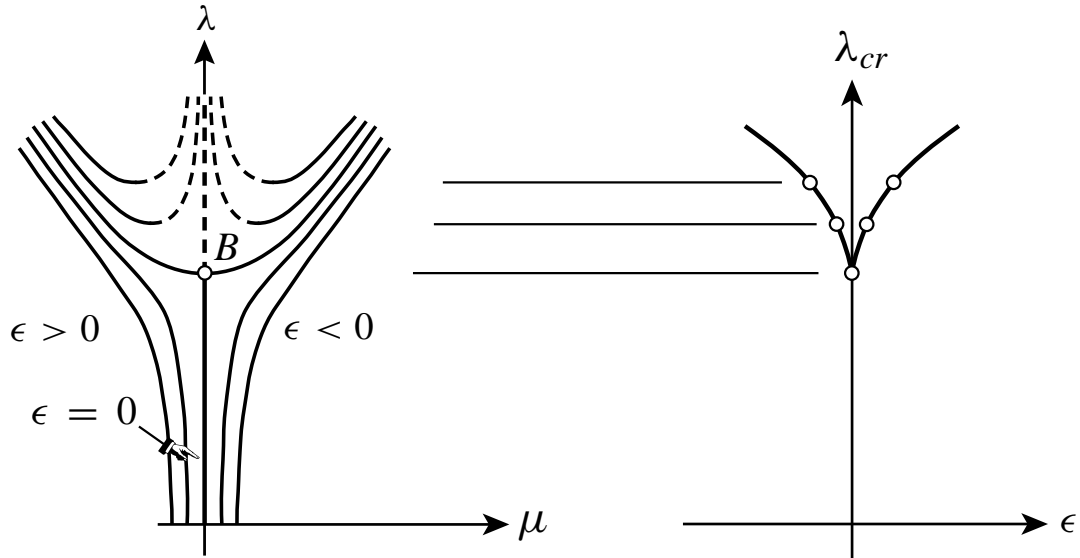


Figure 28.8. Effect of initial imperfections at a stable-symmetric bifurcation point.

critical load level of the perfect system is reached. It follows that there is no local branch of the $\lambda_{cr}(\epsilon)$ curve for $\epsilon < 0$.

§28.5.3. Stable Symmetric Bifurcation

Typical pictures for an stable symmetric point of bifurcation are shown in Figure 28.8. The general behavior is similar to that encountered in the hinged-cantilever example of §25.2. We see that imperfections play here a relatively minor role in changing the response of the system. Small positive and small negative imperfections have similar effects, each yielding a continuously stable and rising equilibrium paths as shown. Therefore, imperfect systems of this type display no sharp failure load, “buckling” being simply characterized by a more rapid growth of the deflections as the critical load of the perfect system is approached.

§28.5.4. Unstable Symmetric Bifurcation

Finally, typical pictures for an unstable symmetric point of bifurcation are shown in Figure 28.9. We see that imperfections play here a significant role in modifying the behavior of the system although the effect is not so drastic as in the asymmetric bifurcation case. Small positive and small negative imperfections have symmetrical effects, each now inducing failure at a limit point that corresponds to a considerably reduced value of $\lambda_{cr}(\epsilon)$. The variation of λ_{cr} with ϵ is shown in the right-hand diagram. For both positive and negative imperfections the function follows locally (that is, near $\epsilon = 0$) the so-called “two-thirds law:”

$$\lambda \propto \epsilon^{2/3}, \quad (28.14)$$

discovered originally by Koiter in the 1940s. This law yields a sharp “cusp” at $\epsilon = 0$ as shown. We can summarize this case as being one of *high imperfection sensitivity* to both positive and negative imperfections.

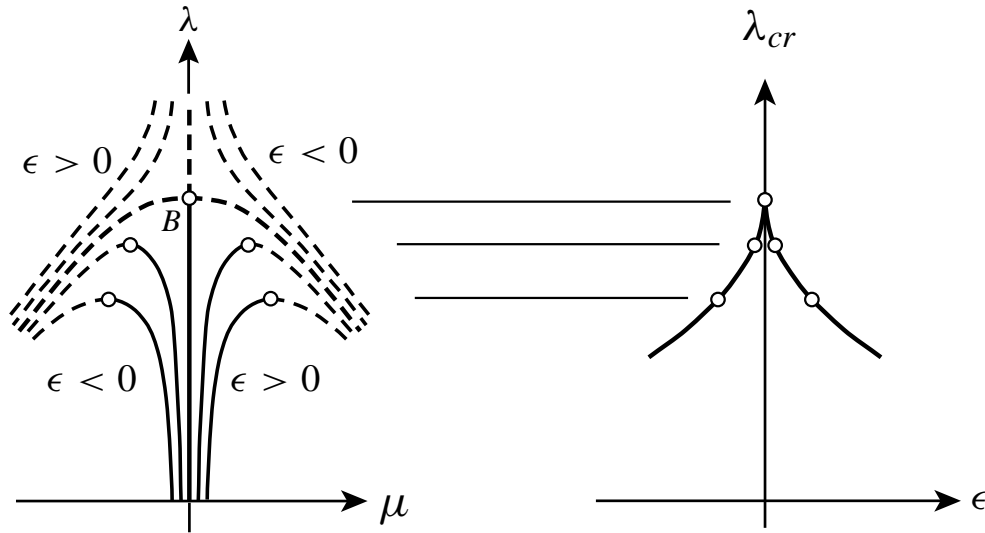


Figure 28.9. Effect of initial imperfections at an unstable-symmetric bifurcation point.

§28.6. Extensions: Multiple Bifurcation, Continuous Systems

The preceding discussion, as well as the treatment of Chapter 24, pertains to limit points and isolated bifurcation points of *discrete* structural systems. This raises questions as to what happens at multiple or compound bifurcation points, or critical points of continuous systems.

At a multiple bifurcation point of order k (order being the rank deficiency of the tangent stiffness matrix there) a second-order analysis similar to that carried out in §27.4 show that one can expect in general 2^k crossing branches. For an isolated bifurcation point $k = 1$ and $2^k = 2$ as previously found. But if $k \geq 2$ much greater complexity of behavior can be expected. At a multiple bifurcation point the effect of initial imperfections is typically far more severe than at single bifurcation points if one or more of the emanating branches are unstable, as is usually the case. The systematic investigation of these effects remains a frontier research subject, which is nonetheless gaining in importance because of its application to stability-optimized aerospace structures that are designed to simultaneously fail in several buckling modes.

As for continuous systems, the aforementioned two-thirds power law for the imperfection sensitivity at an unstable-symmetric bifurcation point carries over to continuous systems if the geometric imperfection is *assumed to have the shape of the buckling mode*. If this common assumption is not made new power laws may emerge from the continuous analysis. As for asymmetric buckling, it remains poorly understood in the continuous case.

Homework Exercises for Chapter 28

Imperfections

EXERCISE 28.1 Work out the details of the analysis of the imperfect propped cantilever described in §28.3. In particular, verify that the diagram shown in Figure 28.5 is correct. Obtain the equation of the imperfection sensitivity diagram $\lambda_{cr}(\epsilon)$ where λ_{cr} are load limits (limit points) obtained when $\epsilon \neq 0$. Plot this diagram for values of $\epsilon = 0$ to 1; note vertical-tangent “cusp” at $\epsilon = 0$! [Qualitatively, the diagram should look like the one in Figure 28.9.]

EXERCISE 28.2 A highly simplified, one-DOF “beer-can-like” structure has the total potential function

$$\Pi(u, f, \epsilon) = U - V, \quad U = kL^2(\sqrt{1 + (u/L)^2} - 1 - \gamma\epsilon)^2, \quad V = fL(1 + (u/L)\epsilon - \sqrt{1 - (u/L)^2}) \quad (\text{E28.1})$$

where u is the state variable, f is the applied load, k , L are structure property constants with dimensions of spring constant and length, respectively, γ is a dimensionless constant, and ϵ is a dimensionless geometric imperfection parameter. Reduce (E28.1) to a dimensionless form

$$\Pi(\mu, \lambda, \epsilon) \quad (\text{E28.2})$$

by defining the state parameter $\mu = u/L$ and the control parameter $\lambda = f/(kL)$, and dividing the whole thing through by kL^2 . From then on take $\gamma = 0$. Form the equilibrium equations and generate a response diagram for the imperfect structure similar to those shown in Figures 28.2 and 28.5, varying ϵ in the range $(-1, 1)$, μ in the range $(-0.99, 0.99)$, and λ in $(0, 1.5)$. From visual inspection conclude whether the structure experiences asymmetric bifurcation (that is, it has a preferred buckling direction) or a symmetric one. Draw the imperfection sensitivity diagram of λ_{cr} versus ϵ . What is the load capacity drop for imperfections of magnitude 0.01, 0.1 and 1?

Using Graphic Tools to Expedite HW

Use of built-in graphic tools such as those provided in Matlab, Mathematica or Maple can speed up significantly the generation of response diagrams for Exercises 28.1 and 28.2. For example, an initial version of the diagram shown in Figure 28.2 was produced by the following Mathematica script:

```
lam[theta_, eps_] := (theta - eps) / Sin[theta];
p1 = Plot[{lam[theta, 0.01], lam[theta, -0.01], lam[theta, 0.1],
  lam[theta, -0.1], lam[theta, 0.2], lam[theta, -0.2], lam[theta, 0.5], lam[theta, -0.5]},
  {theta, -Pi/1.2, Pi/1.2}, PlotRange -> {0, 2}, DisplayFunction -> Identity];
p2 = Plot[lam[theta, 0], {theta, -Pi/1.2, Pi/1.2}, PlotRange -> {0, 2}, DisplayFunction -> Identity];
p3 = Plot[1/Cos[theta], {theta, -1.5, 1.5}, PlotRange -> {0, 2}, DisplayFunction -> Identity];
Show[Graphics[Thickness[0.002]], p1, Graphics[Thickness[0.004]], p2,
  Graphics[Thickness[0.004]], Graphics[AbsoluteDashing[{5, 5}]], p3,
  PlotRange -> {0, 2}, Axes -> True, AxesLabel -> {"theta", "lambda"},
  DisplayFunction -> $DisplayFunction];
```

The plot cell was then converted and saved as an Adobe Illustrator 88 file, picked up by Adobe Illustrator 6.0 and “massaged” for bells and whistles such as Greek labels, dashed lines, shading of unstable region, etc.